J Geophys (1982) 50:171 – 176

Journal of Geophysics

Reflection and Transmission of Love Channel Waves at Coal Seam Discontinuities Computed with a Finite Difference Method*

M. Korn[1] and H. Stöckl[2]

[1] Institut für Meteorologie und Geophysik, Feldbergstr. 47, D-6000 Frankfurt, Federal Republic of Germany
[2] Fraunhofer-Institut für Werkstoffmechanik, Rosastr. 9, D-7800 Freiburg, Federal Republic of Germany

Abstract. Channel waves serve as a tool for the detection of discontinuities in coal seams caused, for example, by tectonic faulting. In this paper we study Love waves propagating along two-dimensional discontinuous coal seams. Synthetic seismograms, computed with an explicit finite difference method, are presented for three types of discontinuities: the seam end, the horizontal and the vertical offset. In all cases the discontinuity reflects mainly those waves with short wavelength and transmits those waves with large wavelength. An additional damping term is introduced into the finite difference formulation in order to prevent reflections from the edges of the computational grid. The boundary conditions at interfaces are all approximated with a truncation error of second order.

Key words: Synthetic seismograms – Finite difference method – Channel waves – Coal seam discontinuities

Introduction

Coals seams are often not continuous but are disturbed by micro-tectonic faults, sand channels or tectonic displacements. For an effective exploitation of a mine it is important to explore such discontinuities in advance. Channel waves are most commonly used to do this (Krey 1963). These waves are radiated from a source located within the coal seam and they are also recorded within the seam. Depending on the geophone setup, either the transmitted or the reflected channel wave is recorded. Marked losses in transmission or the occurrence of a strong reflection indicate the presence of a discontinuity.

For a better understanding of the properties of these waves, it is useful to investigate the reflection and transmission process theoretically. In the past, channel waves of the Rayleigh type were analyzed extensively by model seismic experiments (Dresen and Freystätter 1976; Freystätter and Dresen 1978). In real prospecting, however, mainly channel waves of the Love type are recorded, which are difficult to study by model seismic means. Therefore we construct numerically synthetic seismograms of Love channel waves propagating in discontinuous coal seams. The method used is an explicit finite difference method, which allows the numerical solution of the wave equation in two-dimensional inhomogeneous media. In the past this technique has been successfully applied to numerous wave propagation problems (Alterman and Loewenthal 1972; Boore 1972; Kelly et al. 1976).

In this paper we use a new approximation of the boundary conditions at interfaces, which has some advantage compared to the usual approximation (Alterman and Rotenberg 1969), as will be explained later. In addition we include a damping term into the wave equation which allows us to suppress the artificial reflections from the edge of the computational grid. In the next section these extensions of the finite difference method will be described. In the subsequent section the propagation of a Love wave in a coal seam ending with a discontinuity perpendicular to the bedding plane is discussed and a simple analytical approximation of the frequency dependence of the reflectivity is derived. Some more complicated seam discontinuities are also discussed.

Method of Calculation

The equation of motion in heterogeneous elastic media can be solved with two different kinds of finite-difference schemes. In the so-called "homogeneous formulation", the equation of motion for homogeneous media is solved numerically. At interfaces between media with different elastic parameters the boundary conditions for continuity of stress and displacement have to be fulfilled in addition. The "heterogeneous formulation" (Boore 1972; Kelly et al. 1976) uses the equation of motion in heterogeneous media, where the elastic parameters are arbitrarily space dependent. In this case there is no need to fulfil boundary conditions explicitly. Kelly et al. (1976) showed that these two formulations, when applied to the same problem, produce slightly different results. In our treatment we employ the homogeneous formulation, but use a different approximation of the boundary conditions with a truncation error of second order. With this approximation we are able to generalize the homogeneous formulation, so that it becomes equivalent to a heterogeneous formulation.

We start with the equation of motion for horizontally polarized shear (SH) waves in cartesian coordinates x and z:

$$\rho v_{tt} = \mu(v_{xx} + v_{zz}). \tag{1}$$

ρ is the density, μ is the shear modulus and $v(x, z, t)$ is the displacement. Subscripts t, x, z mean the partial derivatives $\partial/\partial t$, $\partial/\partial x$, $\partial/\partial z$.

The boundary conditions at a horizontal interface at depth $z = a$ are:

$$\mu^{(1)} v_z^{(1)}|_{z=a} = \mu^{(2)} v_z^{(2)}|_{z=a} \tag{2a}$$

$$v^{(1)}|_{z=a} = v^{(2)}|_{z=a} \tag{2b}$$

Here, the indices in brackets denote the different media.

* Contribution No. 241, Geophysikalisches Institut, Universität Karlsruhe

[1, 2] Formerly at: Geophysikalisches Institut, Universität Karlsruhe, Hertzstr. 16, D-7500 Karlsruhe, Federal Republic of Germany

0340-062X/82/0050/0171/$01.20

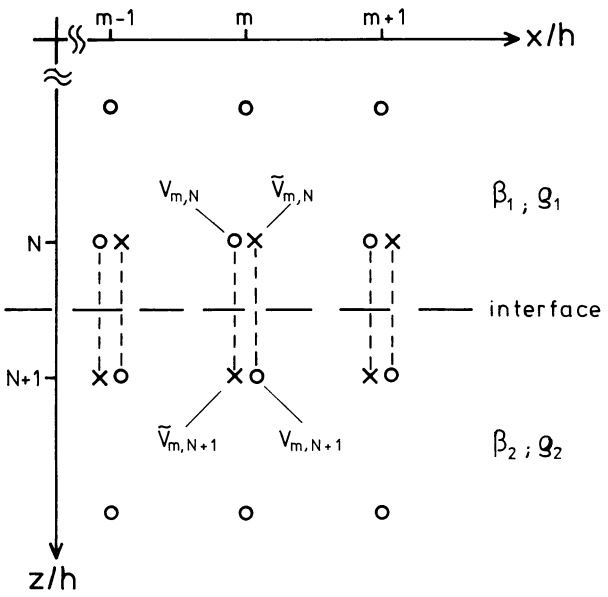

Fig. 1. Arrangement of grid points at a horizontal interface at $z=(N+1/2)h$. Real points are denoted by ○, ficticious points by × The ficticious points below the interface belong to the upper medium and vice versa

For the discretization, a rectangular grid with equal spacings $\Delta x=\Delta z=h$ is employed. The time step is Δt. Using the notation $v(mh, nh, p\Delta t)=v^p_{m,n}$, the well-known finite difference approximation of Eq. (1) with a truncation error of second order is (Boore 1970):

$$v^{p+1}_{m,n}=-v^{p-1}_{m,n}+\left(\frac{\beta\Delta t}{h}\right)^2(v^p_{m+1,n}+v^p_{m-1,n}+v^p_{m,n+1}+v^p_{m,n-1})+2\left[1-2\left(\frac{\beta\Delta t}{h}\right)^2\right]v^p_{m,n} \tag{3}$$

where $\beta=(\mu/\varrho)^{1/2}$ is the shear velocity.

This scheme is numerically stable, if the condition $\frac{\beta\Delta t}{h}\leqq 1/\sqrt{2}$ is fulfilled.

The boundary conditions, Eq. (2) are usually approximated by introducing one line of ficticious grid points at a distance h from the boundary and approximating the derivatives in Eq. (2a) by finite differences with a truncation error of first order (Alterman and Loewenthal 1972). This obviously causes some additional error in the numerical solution.

In our approximation we put an interface between two grid lines N and $N+1$ and add a line of ficticious points on either side of the interface (see Fig. 1). The boundary condition Eq. (2a) is approximated using central differences with respect to the interface at $N+\frac{1}{2}$ resulting in a truncation error of second order:

$$\frac{\mu^{(1)}}{h}\cdot(\tilde{v}^p_{m,N+1}-v^p_{m,N})=\frac{\mu^{(2)}}{h}\cdot(v^p_{m,N+1}-\tilde{v}^p_{m,N}). \tag{4a}$$

Ficticious points are denoted by a tilde.

Equation (2b) is approximated by linear interpolation between neighbouring grid points:

$$\tfrac{1}{2}(v^p_{m,N}+\tilde{v}^p_{m,N+1})=\tfrac{1}{2}(\tilde{v}^p_{m,N}+v^p_{m,N+1}). \tag{4b}$$

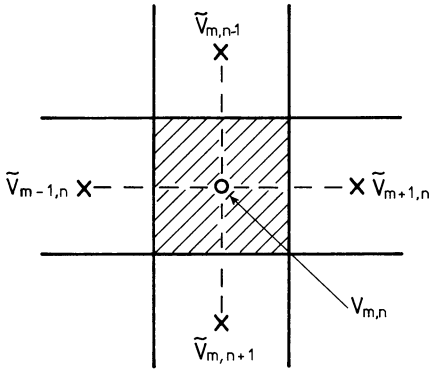

Fig. 2. Arrangement of ficticious grid points (×) in a heterogeneous medium in the neighbourhood of a real point (○) at $x=mh$, $y=nh$. The hatched area indicates the homogeneous region with density $\rho_{m,n}$ and shear velocity $\beta_{m,n}$ surrounding the point (m,n)

Equations (4a) and (4b) can be solved for the unknown ficticious points:

$$\left.\begin{aligned}\tilde{v}^p_{m,N}&=(2v^p_{m,N}+(M-1)v^p_{m,N+1})/(M+1)\\ \tilde{v}^p_{m,N+1}&=(2v^p_{m,N+1}+(M-1)v^p_{m,N})/(M+1)\end{aligned}\right\} \tag{5}$$

with $M=\mu^{(2)}/\mu^{(1)}$.

This formulation can be analogously applied to vertical interfaces and so any interface consisting of horizontal and vertical sections can be modeled.

We now consider a completely heterogeneous medium with velocity $\beta(x,z)$ and density $\rho(x,z)$. In order to apply the above concept of boundary conditions to this case, we assume that each grid point (m,n) is located in the center of a homogeneous quadratic region with parameters $\beta_{m,n}$ and $\rho_{m,n}$ (see Fig. 2). Between every two neighbouring points there exists an interface, where the boundary conditions of Eq. (2) have to be satisfied. The finite difference approximation of the homogeneous wave equation for the grid point (m,n) is, according to Eq. (3):

$$v^{p+1}_{m,n}=-v^{p-1}_{m,n}+\left(\frac{\beta_{m,n}\Delta t}{h}\right)^2(\tilde{v}^p_{m+1,n}+\tilde{v}^p_{m-1,n}+\tilde{v}^p_{m,n+1}+\tilde{v}^p_{m,n-1})+2\left[1-2\left(\frac{\beta_{m,n}\Delta t}{h}\right)^2\right]v^p_{m,n} \tag{6}$$

Note that ficticious points have been used for all neighbouring points. The displacements at the ficticious points can be expressed in terms of real points by using Eq. (5) appropriately for all four boundaries. Equation (6) then becomes

$$\begin{aligned}v^{p+1}_{m,n}=&-v^{p-1}_{m,n}+2v^p_{m,n}+2\left(\frac{\beta_{m,n}\Delta t}{h}\right)^2\left[M_1\cdot(v^p_{m+1,n}-v^p_{m,n})\right.\\&-M_2(v^p_{m,n}-v^p_{m-1,n})+M_3(v^p_{m,n+1}-v^p_{m,n})\\&\left.-M_4(v^p_{m,n}-v^p_{m,n-1})\right]\end{aligned} \tag{7}$$

with

$$M_1=\frac{\mu_{m+1,n}}{\mu_{m,n}+\mu_{m+1,n}};\quad M_2=\frac{\mu_{m-1,n}}{\mu_{m,n}+\mu_{m-1,n}};$$

$$M_3=\frac{\mu_{m,n+1}}{\mu_{m,n}+\mu_{m,n+1}};\quad M_4=\frac{\mu_{m,n-1}}{\mu_{m,n}+\mu_{m,n-1}}$$

We have now obtained a heterogeneous formulation, because Eq. (7) is valid in a medium, in which the elastic parameters

may vary from grid point to grid point. In contrast to the heterogeneous formulation of Boore (1972) and Kelly et al. (1976), Eq. (7) is completely equivalent to the homogeneous formulation (Eqs. (3) and (4)). Furthermore, second order approximations are used throughout the whole scheme.

It is interesting to note that Eq. (7) can also be obtained following the method of Tikhonov and Samarskii (Mitchell 1969), which was also discussed in Boore (1972):

Their approach to the equation of motion in heterogeneous media depends on the detailed variation of $\mu(x, z)$. In this case the coefficients M_1 to M_4 in Eq. (7) have to be replaced by integral formulas, for example

$$M_1 = \frac{h}{2\mu_{m,n}} \cdot \left(\int_{x_m}^{x_{m+1}} \frac{dx}{\mu(x,z)} \right)^{-1} \tag{8}$$

If μ jumps from $\mu_{m,n}$ to $\mu_{m+1,n}$ at $x_{m+\frac{1}{2}}$, Eq. (8) can be integrated and M_1 is the same as in Eq. (7).

A problem which is common to all finite difference computations is the occurrence of reflections from the boundaries of the model. Several methods have been developed to attenuate these edge reflections (Smith 1974; Clayton and Engquist 1977; Reynolds 1978), but none is able to prevent them completely. In this paper our approach is to modify the equation of motion in such a way that the energy is dissipated within the medium. For the models in our study this proved to be a practicable way to suppress disturbing reflections almost completely.

First, Eq. (1) is transformed into the frequency domain and the frequency ω is substituted by the complex frequency $\omega - i\sigma$. Transformation back into the time domain yields a modified equation of motion:

$$v_{tt} + 2\sigma v_t + \sigma^2 v = \beta^2 (v_{xx} + v_{zz}) \tag{9}$$

Solutions of Eq. (9) describe the propagation of waves with a dissipation factor $e^{-\sigma t}$, or, what is equivalent, $e^{-\frac{\sigma}{\beta} r}$ (r = distance traveled by the wave). This means that after a distance $r_0 = \beta/\sigma$ the amplitude of a plane wave has decreased by a factor of e^{-1}. Suppressing of edge reflections is now achieved by including a zone with nonvanishing σ along the boundaries of the grid. This zone has to be so large that the amplitudes of waves passing it twice become negligible. In order to avoid additional reflections from the boundary separating the elastic medium with $\sigma = 0$ and the dissipating medium with $\sigma > 0$ we made σ space dependent and let it increase linearly with the distance from the boundary of the elastic medium.

It should be noted that Eq. (9) implies a specific dissipation function Q proportional to frequency and hence a strong frequency dependence of dissipation. Therefore, it is normally not suited for realistic modeling of dissipative wave propagation in seismic media, but only for the suppression of unphysical reflections.

The finite difference approximation of Eq. (9) in a heterogeneous medium is obtained in the same way as shown before for the elastic wave equation. The difference equation corresponding to Eq. (7) becomes

$$\begin{aligned} v^{p+1}_{m,n} = (\sigma_{m,n}\Delta t + 1)^{-1} \Big\{ & (\sigma_{m,n}\Delta t - 1) v^{p-1}_{m,n} + 2 \left(\frac{\beta_{m,n}\Delta t}{h} \right)^2 \\ & [M_1 (v^p_{m+1,n} - v^p_{m,n}) - M_2 (v^p_{m,n} - v^p_{m-1,n}) \\ & + M_3 (v^p_{m,n+1} - v^p_{m,n}) - M_4 (v^p_{m,n} - v^p_{m,n-1})] \\ & + 2[1 - \sigma_{m,n}\Delta t] v^p_{m,n} \Big\} \end{aligned} \tag{10}$$

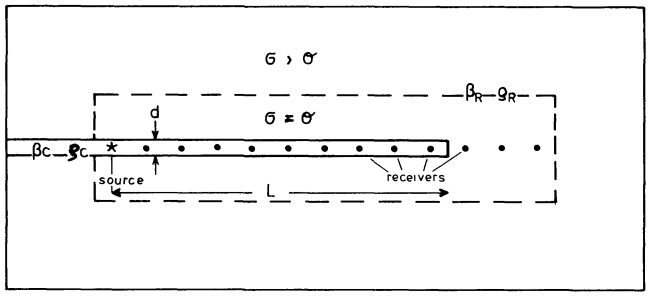

Fig. 3. Geometry of the computational model. The dashed line indicates the boundary between the elastic medium ($\sigma = 0$) and the dissipating medium ($\sigma > 0$). The grid size was 250×80 grid points. The grid spacing h was 0.5 m

With this method the amplitudes of the edge reflections are attenuated to about 3% of the incident amplitudes, if the zone with slowly increasing σ is about 25–30 h thick.

Results

Reflection and Transmission of Love Waves at the End of a Coal Seam

The first model which we will study in detail is a coal seam with thickness $d = 2.5\,m$, shear velocity $\beta_c = 1$ km/s and density $\rho_c = 1.5\,\mathrm{g/cm^3}$, embedded in homogeneous rock with $\beta_R = 2$ km/s and $\rho_R = 3\,\mathrm{g/cm^3}$. A line source is located in the middle of the seam. After the horizontal distance $L = 20.5d$ from the source the seam ends with a discontinuity perpendicular to the bedding plane. The geometry of the computational model is given in Figure 3. The source radiates a pulse $s(t) = \sin(2\pi t/T_s) - \frac{1}{2}\sin(4\pi t/T_s)$ for $0 < t < T_s$. T_s is the pulse duration.

Figure 4 shows seismogram sections for two different pulse lengths T_s. The receivers are located at the same depth as the source and at various horizontal distances x from the source. In Fig. 4a the dominant wavelength in the seam is four times the seam thickness d, in Fig. 4b it is reduced to $2.5d$. The dispersion of the direct seam wave is clearly seen, resulting in an Airy-phase with large amplitudes in the second example.

Having passed the discontinuity at $x = L$, the wave propagates in the rock as a body wave without further dispersion. The reflected seam wave shows strong frequency dependence. In Fig. 4a, only a weak reflection can be seen, whereas for the higher frequencies in Fig. 4b the reflected amplitudes become fairly large, especially in that part of the seismogram containing the Airy-phase. A reflection coefficient R and a transmission coefficient T, which are defined as follows, show this in more detail. R (T) is the maximum peak-to-peak amplitude of the reflected (transmitted) wave, measured at a distance $x = 0.5L$ ($x = 1.5L$). Both R and T are normalized with respect to the amplitude of the wave coming directly from the source, measured at $x = 0.5L$. Figure 5 shows R and T as a function of the dominant wavelength of the direct wave. Obviously R increases for higher frequencies, while T dominates at low frequencies. Waves which are very long compared to the seam thickness, are not reflected at all. Figure 5 gives rough information about the frequency range that should be used for the optimal detection of discon-

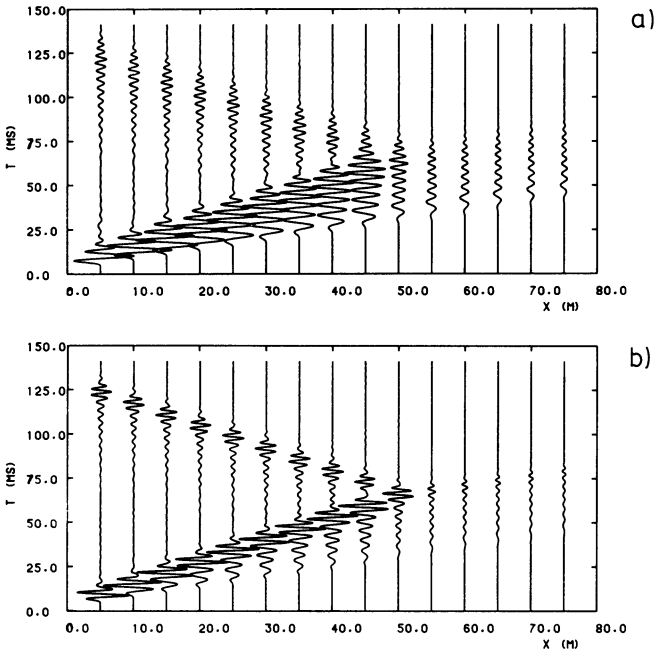

Fig. 4a, b. Seismogram sections for the model of Fig. 3. The duration T_s of the source pulse is **a** 10 ms and **b** 6.25 ms. $L=50$ m

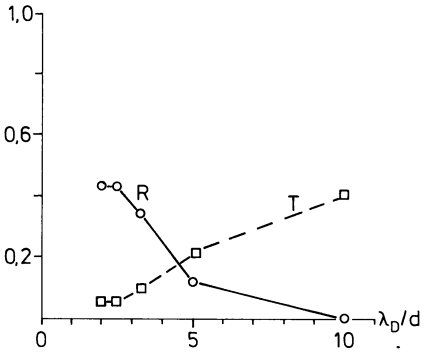

Fig. 5. Reflection coefficient R and transmission coefficient T of the seam end (model of Fig. 3) as defined in the text versus the dominant wavelength λ_D in the seam

tinuities. In this case, wavelengths of up to $2\text{-}3d$ produce maximal reflection and minimal transmission.

In order to get more detailed information about the frequency dependence of the reflection and transmission process, we compute the reflectivity function $r(\omega)$ and the transmissivity function $t(\omega)$ from the amplitude spectra of the three waves taken at the points mentioned above. $r(\omega)$ and $t(\omega)$ are shown in Fig. 6, $r(\omega)$ behaving like a high-pass filter. It approaches zero for low frequencies and goes up to a maximum of about 0.55 for high frequencies. The transmissivity $t(\omega)$, in contrast, drops to a small but constant value at high frequencies.

In addition to these numerical results we derive in the following a simple analytical approximation for the reflectivity $r(\omega)$. It shows on which parameters the reflection process mainly depends.

Figure 7 gives the amplitude distribution $A(z)$ of a plane harmonic fundamental-mode Love wave in a layer between two identical homogeneous half-spaces for various frequencies. $z=0$ denotes the middle of the layer and d is its thickness. $A(z)$ is given by

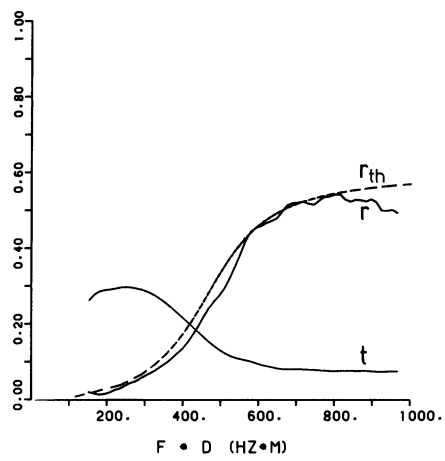

Fig. 6. Reflectivity r together with its analytical approximation r_{th} and transmissivity t versus fd for the model of a seam end

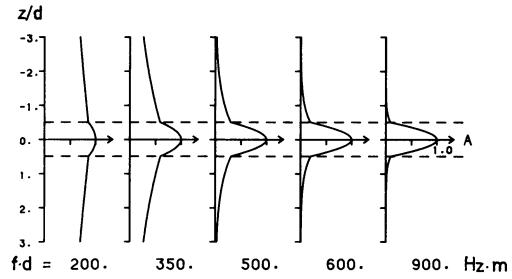

Fig. 7. Amplitude distribution for plane harmonic Love waves (fundamental mode) in a layer between two identical halfspaces for various frequencies

$$A(z)=\begin{cases}A_0\cos(k\gamma_1 z) & |z|\leqq d/2\\ A_0\cos(k\gamma_1 d/2)\exp\left[-k\gamma_2(|z|-d/2)\right] & |z|>d/2\end{cases} \tag{11}$$

with

$$\gamma_1=(c^2/\beta_c^2-1)^{1/2};\quad \gamma_2=(1-c^2/\beta_R^2)^{1/2}$$

$c(\omega)$ is the phase velocity and k is the wave number. For higher frequencies, the amplitudes become more and more concentrated within the layer, as shown in Fig. 7. We now assume that only that part of the wave propagating inside the layer is reflected at the discontinuity with the reflection coefficient for plane waves $r_0=(\rho_c\beta_c-\rho_R\beta_R)/(\rho_c\beta_c+\rho_R\beta_R)$.

Moreover, the amplitudes in the neighbouring rock are supposed to be not affected by the discontinuity. Under this assumption, an approximation for the reflectivity $r(\omega)$ can be written as

$$r_{th}(\omega)=r_0\cdot\int_{-d/2}^{+d/2}A(z)\,dz\Big/\int_{-\infty}^{+\infty}A(z)\,dz \tag{12}$$

Inserting Eq. (11) into Eq. (12) and making use of the dispersion relation for Love waves in a layer of thickness $d/2$ over a halfspace,

$$\tan\left[\omega\frac{d}{2}\cdot(\beta_c^{-2}-c^{-2})^{1/2}\right]=\mu_R\gamma_2/\mu_c\gamma_1$$

the final result is

$$r_{th}(\omega)=r_0\Big/\left(1+\frac{\mu_c(\beta_c^{-2}-c^{-2})}{\mu_R(c^{-2}-\beta_R^{-2})}\right) \tag{13}$$

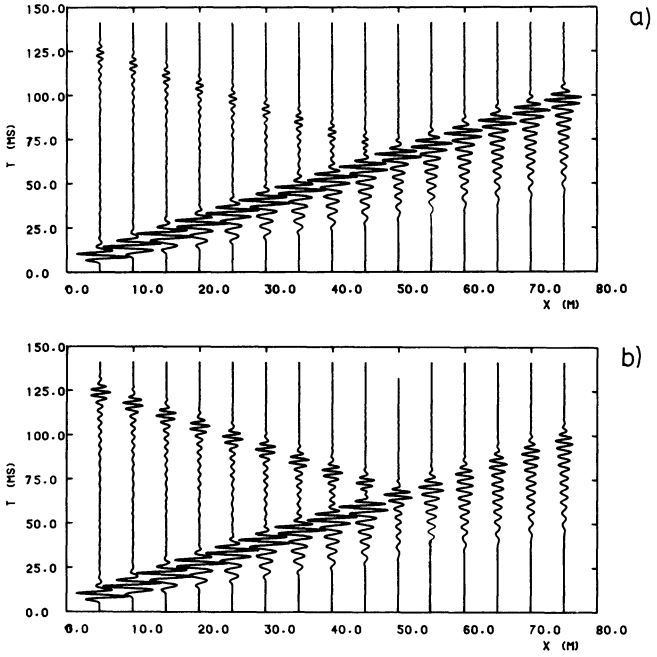

Fig. 8a, b. Seismogram sections for the model with a vertical seam offset b at $x=50$ m. The duration of the source pulse is 6.25 ms. Seam thickness $d=2.5$ m. **a** $b=0.4d$, **b** $b=d$

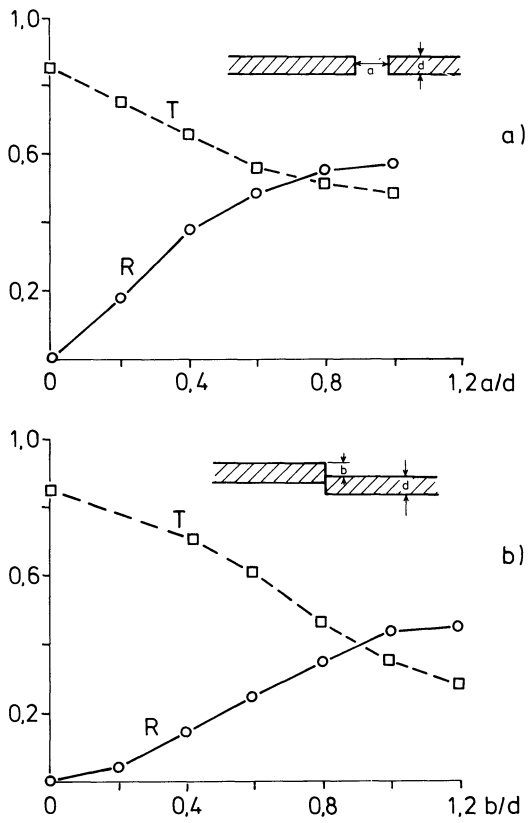

Fig. 9a, b. Reflection coefficient R and transmission coefficient T versus **a** the horizontal offset a with $b=0$ and **b** the vertical offset b with $a=0$

$r_{th}(\omega)$ is shown in Fig. 6. It agrees with the numerically obtained result to within a few per cent over the whole range of frequencies. From this we may conclude that the amplitude of the reflected Love wave depends mainly on the amplitude partition of the incident wave between rock and coal, and that other effects, such as diffractions at the seam corners, are not important in this case.

Horizontal and Vertical Offsets

In this section we will discuss the reflection and transmission of Love waves at more realistic seam discontinuities. The intrusion of a sand channel, for example, may be simulated by a horizontal offset. Similarly, a tectonic fault may result in a vertical offset of the seam. We compute seismogram sections for different values of the horizontal offset a and vertical offset b. From the seismograms the reflection and transmission coefficients R and T and the reflectivity and transmissivity functions $r(\omega)$ and $t(\omega)$ are obtained as described before. The elastic parameters and the seam thickness are the same as in the previous section. The source time function is the same in all cases with a dominant wavelength $\lambda_D=\beta_c \cdot T_s=2.5d$.

In Fig. 8, two seismogram sections with different values of the vertical offset b can be compared: $b=0.4d$ and $b=d$, respectively. In the first case the reflected seam wave is weak, and the transmitted wave is nearly unaffected by the discontinuity. In the second example, however, the reflected wave is quite strong, whereas the transmitted wave is relatively weak, particularly in that part of the seismograms dominated by the high-frequent Airy-phase. From this example we may conclude that offsets of less than one half of the seam thickness can barely be detected by seam wave observations.

The reflection and transmission coefficients for both horizontal and vertical offsets are drawn in Fig. 9. (We do not show seismogram sections for horizontal offsets, because they look very similar to those in Fig. 8). For horizontal offsets the reflection coefficients are always greater than for the corresponding vertical offsets. The transmission coefficients are not so different in the two cases. Only for offsets of about one seam thickness or more, are the transmission coefficients for a vertical offset significantly smaller than those for a horizontal offset. Apparently, reflected seam waves are more sensitive to discontinuities with a horizontal offset than to discontinuities with a vertical offset. Suppose a reflection coefficient of about 0.5 is regarded as sufficient for a clear identification of a reflected seam wave, then a horizontal offset of about $0.5d$ could be detected, whereas a vertical offset of $1d$ would be needed to produce the same reflection coefficient. The seam wave transmitted through the discontinuity, however, is more attenuated in the case of a vertical offset, if the offset is at least $1d$. Therefore a large vertical offset may be more easily detected with the aid of transmission measurements.

Finally we look at the reflectivity and transmissivity functions for some special cases. Figure 10 gives $r(\omega)$ and $t(\omega)$ for the seismogram sections with a vertical offset already shown in Fig. 8. For the large offset of one seam thickness in Fig. 10b the reflectivity grows with frequency up to a maximum of about 0.6, while the transmissivity drops sharply for frequencies of more than $450/d$ Hz. This is due to the fact that for higher frequencies the amplitudes of the incident wave become more and more concentrated within the seam and therefore a higher percentage of the incident energy is reflected at the discontinuity. If the vertical offset is less than $1d$, as in Fig. 10a, the two parts of the seam overlap at the discontinuity and the incident energy propagating inside the

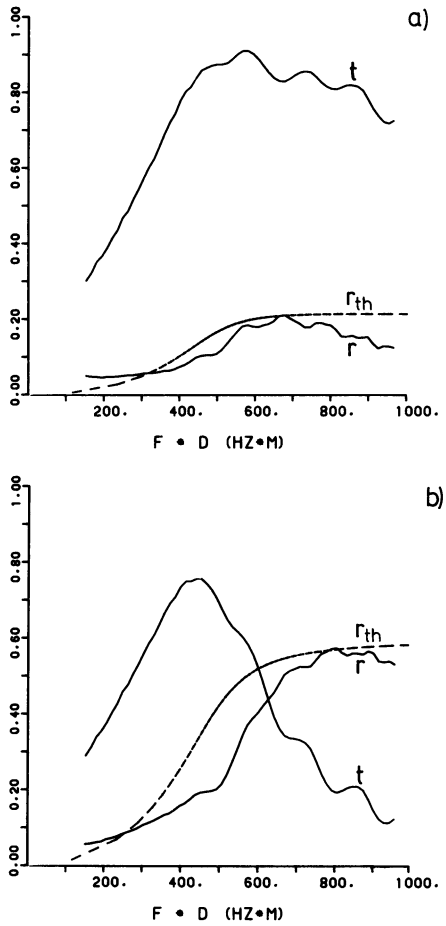

Fig. 10a, b. Reflectivity r together with its analytical approximation r_{th} and transmissivity t versus fd for the model with a vertical seam offset **a** $b=0.4d$ and **b** $b=d$

seam is only partially reflected. Therefore the reflectivity is small over the whole range of frequencies and the transmissivity is only slightly reduced at high frequencies.

For the models with a horizontal offset we obtained reflectivity and transmissivity functions which differ only slightly from those for vertical offsets. The general feature in all cases is an increase of the reflectivity and a decrease of the transmissivity with frequency. As a consequence it seems not to be possible to use spectral analysis of the reflected and transmitted seam waves to distinguish between different types of discontinuities.

For the models with a vertical offset it is possible to compute the analytical approximation $r_{th}(\omega)$ for the reflectivity function. r_{th} is obtained according to Eq. (12) with the difference that integration over $A(z)$ in the numerator is carried out not from $-d/2$ to $+d/2$ but over that depth range, where a discontinuity is actually present in the special model. The approximation r_{th} is additionally given in Fig. 10. It follows that even for these rather complicated models r_{th} predicts correctly the order of magnitude of the reflectivity.

Summary and Conclusions

An explicit finite difference scheme has been presented for the solution of the equation of motion in heterogeneous media, which has the following advantages compared to commonly used schemes:

(1) The boundary conditions at interfaces are all approximated with a truncation error of second order. Furthermore, this scheme is developed into a heterogeneous formulation with the same accuracy.

(2) A damping mechanism is included which attenuates waves approaching the edges of the computational grid and thus almost completely prevents edge reflections.

With this scheme the propagation of Love waves in coal seams with discontinuities was calculated. We restricted ourselves to some simple discontinuities such as horizontal and vertical offsets, although it is possible to treat more complicated models with the same finite difference scheme.

The reflection and transmission process at a discontinuity depends strongly on the frequency range of the incident Love wave. As a general result, it was found that low frequencies are mainly transmitted and high frequencies are mainly reflected. This is explained qualitatively by the amplitude partition of Love waves between rock and coal as a function of frequency. For the vertical offset we derive an analytical approximation for the reflectivity as a function of frequency, which agrees satisfactorily with the numerical results.

The study predicts the amount of the offset which may be detected for a given detection level and a given dominant wavelength. The best results are obtained with dominant wavelengths up to about 3 seam thicknesses. The reflectivity and transmissivity functions differ slightly for different types of discontinuities, but probably not enough to allow for a discrimination in practice.

Acknowledgements. We thank G. Müller for helpful comments and for reading the manuscript and I. Hörnchen for typing it. The computations were performed at the computing centers of the Universities of Karlsruhe and Frankfurt.

References

Alterman, Z., Rotenberg, A.: Seismic waves in a quarter plane. Bull. Seismol. Soc. Am. **59**, 347–368, 1969

Alterman, Z., Loewenthal, D.: Computer generated seismograms. In: Methods in computational physics, Vol. 12, B. Bolt, B. Alder, S. Fernbach, M. Rotenberg, eds. New York: Academic Press 1972

Boore, D.M.: Love waves in nonuniform waveguides: finite difference calculations. J. Geophys. Res. **75**, 1512–1527, 1970

Boore, D.M.: Finite difference methods for seismic wave propagation in heterogeneous materials. In: Methods in computational physics, Vol. 11, B. Alder, S. Fernbach, M. Rotenberg, eds. New York: Academic Press 1972

Clayton, R., Engquist, B.: Absorbing boundary conditions for acoustic and elastic wave equations. Bull. Seismol. Soc. Am. **67**, 1529–1540, 1977

Dresen, L., Freystätter, S.: Rayleigh channel waves for the in-seam seismic detection of discontinuities. J. Geophys. **42**, 111–129, 1976

Freystätter, S., Dresen, L.: The influence of oblique-dipping discontinuities on the use of Rayleigh channel waves for the in-seam seismic reflection method. Geophys. Prosp. **26**, 1–15, 1978

Kelly, K.R., Ward, R.W., Treitel, S., Alford, R.M.: Synthetic seismograms: a finite difference approach. Geophysics **41**, 2–27, 1976

Krey, T.C.: Channel waves as a tool of applied geophysics in coal mining. Geophysics **28**, 701–714, 1963

Mitchell, A.R.: Computational methods in partial differential equations. New York: J. Wiley 1969

Reynolds, A.C.: Boundary conditions for the numerical solution of wave propagation problems. Geophysics **43**, 1099–1110, 1978

Smith, W.D.: A nonreflecting plane boundary for wave propagation problems. J. Comp. Phys. **15**, 492–508, 1974

Received September 16, 1981; Revised version October 26, 1981
Accepted October 27, 1981